NRL REPORT 3612

STANDING-WAVE MEASURING EQUIPMENT FOR MICROWAVES

P. A. Portmann

January 17, 1950

Approved by:

Dr. L. C. Van Atta, Head, Antenna Research Branch
Dr. J. M. Miller, Superintendent, Radio Division I

NAVAL RESEARCH LABORATORY
CAPTAIN F. R. FURTH, USN, DIRECTOR
WASHINGTON, D.C.

DISTRIBUTION

CNO	1
BuAer	
Attn: Code EL-51	1
BuOrd	
Attn: Code Re4f	1
BuShips	
Attn: Code 833	1
ONR	
Attn: Code 427	1
Attn: Code 470	1
CO, USNPG, Dahlgren	1
Dir., USNEL	2
Attn: Code 300	1
Dir., USNUSL	
Attn: Mr. C. M. Dunn	1
CO, NADS	
Attn: Dr. H. Krutter	1
Attn: Mr. E. Steele	1
Attn: Mr. E. R. Schlieben	1
CDR, USNOTS	
Attn: Reports Unit	2
BAGR, CD, Wright-Patterson AFB	
Attn: CADO-D1	1
Supt., USNPGS	1
CO, NATC	
Attn: Mr. L. S. Marquardt	2
OCSigO	
Attn: SIGGC-R-2	1
Attn: Mr. A. R. Beach	1
Attn: Ch. Eng. & Tech. Div., SIGTM-S	1
CO, SCEL	
Attn: Dir. of Eng.	2

Dir., ESL	
Attn: Mr. O. C. Woodyard	1
Attn: Mr. Leonard Moore	1
CO, Hdqs., Strategic Air Command, Air Base	
Attn: Electronics Section	1
Chief of Staff, USAF	
Attn: AFMEN-2	1
CG, AMC, Wright-Patterson AFB	
Attn: Major J. E. Lambert, MCREEP	1
Attn: Mr. T. J. Gibbons, MCREEO	1
Attn: Mr. R. E. Kester, MCREER	1
Attn: Mr. A. L. Bell, MCREER	1
Attn: Mr. G. Rappaport, MCREER	1
Attn: Eng. Div., Electronics Subdiv., MCREEO-2	1
CO, Cambridge Air Force Research Laboratories	
Attn: Dr. R. C. Spencer	1
Attn: Mr. R. M. Barrett	1
Attn: ERRS	1
CO, Watson Labs., AMC, Red Bank	
Attn: ENR	1
Office of Tech. Services, Dept. of Commerce	2
Dir., NBS	
Attn: CRPL	1
RDB	
Atttn: Library	2
Attn: Navy Secretary	1
Attn: Committee on Electronics	1
Naval Res. Sec., Science Div., Library of Congress	
Attn: Mr. J. H. Heald	2

NAVY-DPPO PRNC. WASH., D.C.

CONTENTS

ABSTRACT

Standing-wave methods of making impedance measurements in the microwave region have been investigated to find means of increasing operating convenience and to reduce the time required in taking readings. Improvements can be made in manually operated instruments by the use of a broad-band transition between the pickup probe and a bolometer detector and by a direct reading phase scale, calibrated as a function of frequency. Data from these instruments are obtained rapidly, and in a form convenient for introduction on an impedance chart. The performance of the improved hand-operated equipments indicates that the techniques could profitably be incorporated in new equipment designs.

The problem of improving the reading time required to obtain standing-wave ratios leads to the consideration of semi-automatic instruments which display the entire standing-wave pattern on a line by means of an oscilloscope. Motorized equipments used for this purpose are a rotating standing-wave detector and an oscillating waveguide phase shifter. Difficulties with both electrical and mechanical features make these instruments impractical. Two other phase-shifter schemes investigated are a rotary phase shifter and a rotary reactor based on the principle of wave propagation in circular guide in the presence of a dielectric strip. Both of these systems operate satisfactorily in terms of instrumentation and data presentation. Improvements in the reflection and transmission coefficient characteristics of the dielectric components are expected to result in satisfactory performance over wide frequency ranges. However, other impedance measuring methods based on isolated traveling waves, rather than standing-wave information may prove to be more amenable to instrumentation for rapid indication.

PROBLEM STATUS

This report concludes one phase of the work on Problem R09-44R; work on other phases is continuing.

AUTHORIZATION

NRL Problem R09-44R
NR 534-033

STANDING-WAVE MEASURING EQUIPMENT FOR MICROWAVES

INTRODUCTION

In the microwave field there exists a general need for equipment to simplify impedance measurements. In particular, there is need for simple equipment yielding moderate accuracies along with rapid data presentation. The purpose of this report is to explore the possibilities of building such equipment based upon conventional standing-wave measuring techniques.

Such techniques have been discussed in a number of papers (References 1, 2, and 3); others contain construction details of various types of instruments (References 4, 5, 6, 7, and 8). The accuracy of measurements made with these equipments has also been discussed in these papers, particularly in References 7 and 8.

Limitations of Present Standing-Wave Techniques and Equipments

Standing-wave instruments in general use consist of a slotted section of transmission line and a movable probe which is connected to a detector through a tuning unit. A scale and vernier is usually provided for use in the measurement of phase. Such equipments have characteristics which limit both their utility and reading speed. The scale and vernier, for example, cannot provide a rapid means of determining phase data since extensive computations are required before data in terms of phase angles can be determined. If adequate detector response is to be obtained, the tuning unit must be readjusted for each frequency used; this tuning operation consumes considerable time compared to that required to take the necessary readings. These time-consuming operations may be avoided by more careful consideration of basic equipment designs which are discussed in the next section of this report.

Since the standing-wave ratio is obtained by moving the detector along the line to points of maximum and minimum response in sequence, the two values and hence the value of their ratio cannot be determined with any degree of rapidity with hand-operated equipment. The process of adjusting a load is further complicated by the fact that the complex standing-wave ratio varies in both amplitude and phase during an adjustment. It is for these reasons that semi-automatic instruments were deemed necessary for a more satisfactory solution to the problem of rapid indication of standing-wave ratio. A number of semi-automatic equipment designs are discussed in the third section of this report.

A last limitation of these equipments stems directly from the technique of standing-wave measurements. Since information is obtained as a standing-wave ratio, a transformation is necessary to obtain both impedance and reflection coefficient information. The

process of transforming can most easily be made by means of a Smith or reflection coefficient chart; the disadvantage is that the transformation must be made manually.

MANUALLY OPERATED EQUIPMENT

Any means available for eliminating the computations involved in obtaining phase data or the need for detector tuning would be a step toward increasing the reliability, speed, and convenience of hand-operated impedance measuring equipment.

Phase Calibrations

One means of eliminating the need for calculations in order to determine phase has already been described (Reference 9). The system consists of a mechanical linkage which automatically transforms the detector position into phase as a mechanical angle. Appropriate corrections are introduced in order to take frequency dependence into account.

An alternative means of avoiding phase computations would be to provide a calibrated scale of phase vs. detector position as a function of frequency. A standing-wave detector provided with such a scale is shown in Figure 1. The unit illustrated is an experimental model which provides only a fixed reference-terminal plane; a more sophisticated design would be one which provides an adjustable-terminal plane by permitting the movement of the scale plate with respect to the transmission line. The necessary phase scale calibration may be obtained by computation or may be found experimentally in terms of

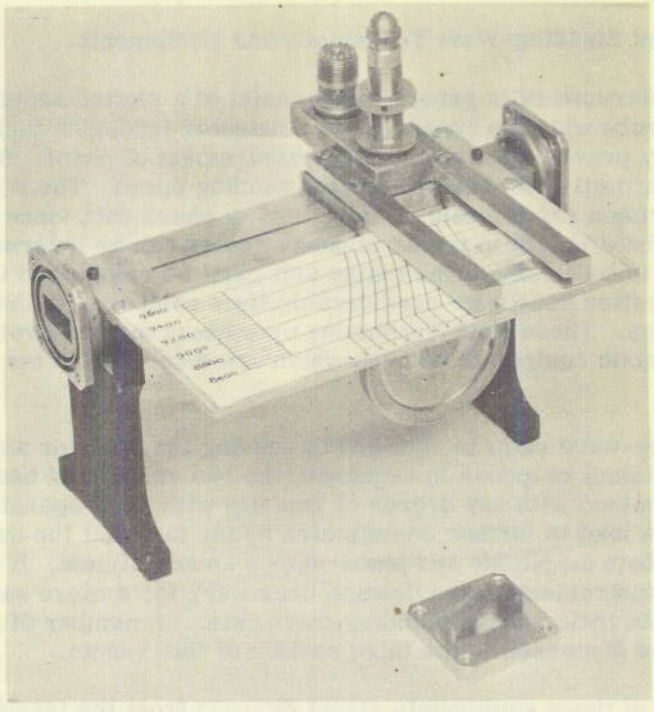

Figure 1 - Standing-wave detector with calibrated phase scale and short circuit plate

short-circuit conditions on the line. A short-circuit plate used for this purpose is also shown in Figure 1.

Broad-Band Probe

To eliminate the need for tuning the output detector, a broad-band probe to waveguide transition was designed to accommodate available broad-band bolometer detectors (References 10 and 11). By not incorporating the detector in the assembly, it is also possible to make use of several different detector types with the same basic instrument. Such a standing-wave detector is shown in Figure 2; a drawing of the transition is shown in Figure 3.

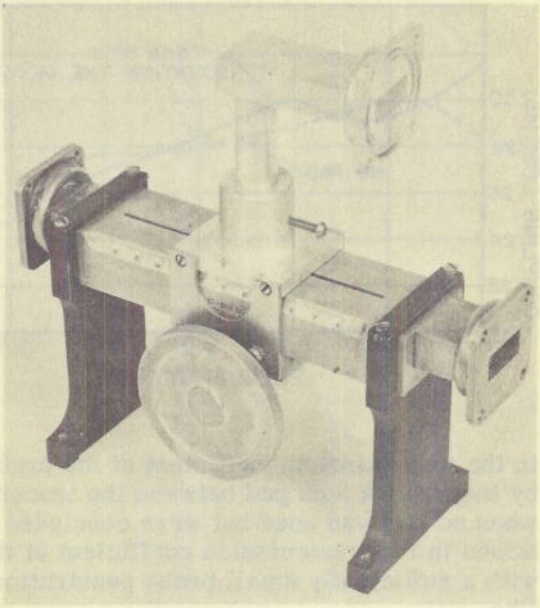

Figure 2 - Standing-wave detector with broad-band transition

Evaluation

No composite instrument making use of the phase scale and broad-band transition features has been constructed; data on the performance of each of these features, however, are available. The relative accuracy of the phase scale was obtained; with the system used errors of 0.02 λ were found. These tests were conducted on a single instrument whose scale had been calibrated in terms of a short circuit. Data were taken directly from the calibrated scale and compared with the results obtained from computed values derived from the numerical values found by means of the scale and vernier on the same instrument. The problem of obtaining sufficiently good reading accuracy is thus very much dependent upon the calibration accuracy and the resolution capability of the phase scale. On the unit tested, the scales were too short for adequate resolution; this would not be the case at longer wavelengths, i.e., approximately 6 cm and longer. At shorter wavelengths than this, however, a mechanical amplification would be desirable to increase the resolution. With such an arrangement reading accuracies of better than 0.005 λ could be obtained without too much difficulty.

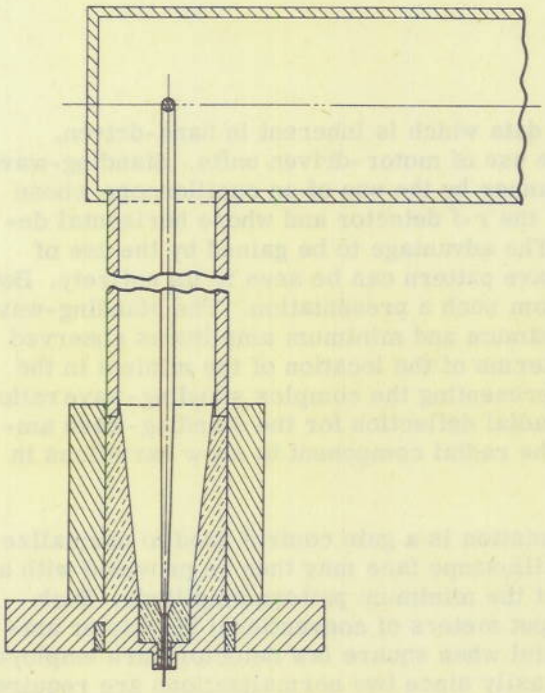

Figure 3 - Broad-band transition and probe

Figure 4 illustrates the variations in the transmission coefficient of the broad-band transition over a frequency range of 12 percent. The detector used for these tests was a Sperry type 82X mount and an 8-ma Barretter element. Variations of ± 4 db were observed

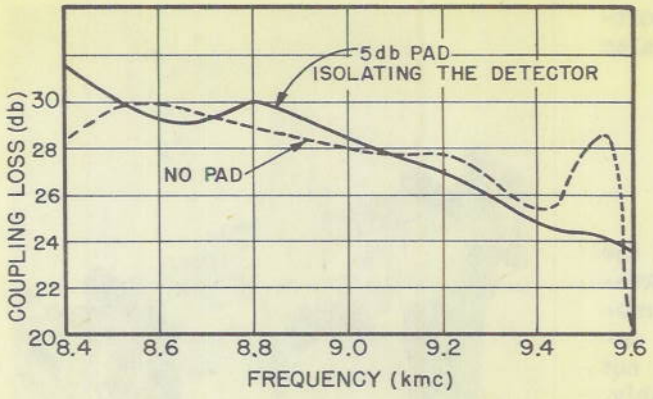

Figure 4 - Coupling of broad-band probe and fixed transition

in the transmission coefficient of the probe and transition section. These data were obtained by inserting a 5 db pad between the transition and detector. Larger variations were observed when no pad was used but were concluded to be due to detector mismatch rather than variations in the transmission coefficient of the transition. Adequate sensitivity was obtained with a sufficiently small probe penetration to minimize the effects of probe reactance in the line.

The results of this preliminary work on manual standing-wave detectors seem to indicate that further effort in this field is needed. In all probability, precision measurements of microwave loads will continue to be made by means of these instruments in the immediate future.

SEMI-AUTOMATIC EQUIPMENT

Presentation of Standing-Wave Data

The lack of flexibility in reading amplitude data which is inherent in hand-driven, standing-wave detectors can be overcome by the use of motor-driven units. Standing-wave data may be presented in a continuous visual manner by the use of an oscilloscope whose vertical deflection is controlled by the output of the r-f detector and whose horizontal deflection is controlled by the detector position. The advantage to be gained by the use of oscilloscope presentation is that the standing-wave pattern can be seen in its entirety. Both standing-wave ratio and phase are obtainable from such a presentation. The standing-wave ratio (r) is calculated from the ratio of the maximum and minimum amplitudes observed in the pattern, while phase (θ) can be found in terms of the location of the minima in the horizontal direction. An alternative method of presenting the complex standing-wave ratio by means of an oscilloscope would be to use a radial deflection for the standing-wave amplitude variations and angular displacement of the radial component to show variations in detector position or phase.

A desirable feature for oscilloscopic presentation is a gain control used to normalize the maximum amplitude of the pattern. The oscilloscope face may then be provided with a scale which reads voltage standing-wave ratio at the minimum pattern amplitude. Such scales have been employed commonly in the output meters of conventional bolometer amplifiers (Reference 3), and are particularly useful when square law detectors are employed. The determination of phase cannot be made as easily since two normalizations are required for most systems; others requiring only one phase-data normalization will be discussed at the conclusion of this section. The normalizations required are, first, to compensate for

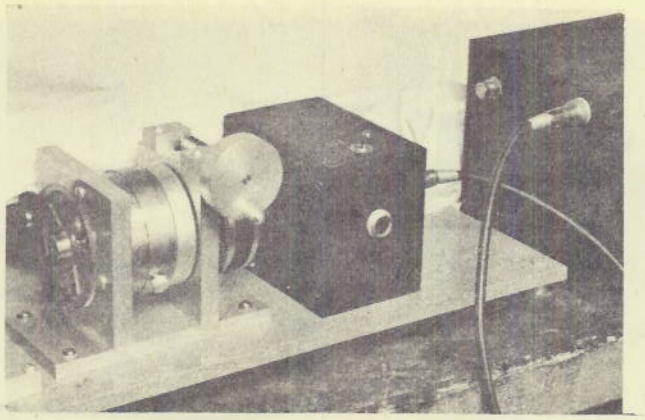

Figure 5 - Calibrated phase-base generator

the length of the phase scale as a function of frequency and, second, to locate the point of zero phase at the measuring position as a function of frequency.

Three means have been employed to transfer phase data to the oscilloscope. The first such equipment makes use of a continuously rotatable potentiometer provided with a d-c bias voltage (Figure 5). The length of the phase scale is controlled by a change in the bias voltage while phase zero normalizations are made by rotating the body of the potentiometer independently of the slider. The second equipment makes use of a trigger voltage to initiate the start of the horizontal trace at an arbitrary point in the standing-wave detector cycle. Equipment consisting of a variable reluctance pickup, a trigger circuit, a saw tooth generator and amplifier is shown in Figure 6-a. With this unit a normalization of the phase scale length is made by adjusting the output amplifier gain control (Figure 6-b). The zero-reference normalization can be made by moving the reluctance pickup with respect to a zero position in the mechanical cycle. The third equipment was used for polar pattern presentation and utilized a synchro data transmission system. The application of this equipment is restricted to systems in which phase is automatically normalized with respect to frequency. A discussion of this property concludes this section.

A comparison of these three equipments in the laboratory has indicated that the potentiometer scheme and the synchro data-transmission system are satisfactory. The trigger circuit, on the other hand, was found to require a very constant speed mechanical drive; small fluctuations in speed showed up as a jitter at one end of the time base on the oscilloscope.

In spite of the number of normalizations involved, this type of presentation affords a considerable saving in reading time over that of conventional hand-operated equipments. In particular, the difficulty of adjusting networks or of matching loads is considerably reduced.

Any system making use of cathode ray tube presentation is limited in the reading accuracy attainable; thus the use of such presentation as a means of measurement must be restricted to less accurate types of work. In all fairness, however, it must be pointed out that the r-f components used are often the limiting factors in the accuracy attainable with this type of system.

In the following subsections, the oscilloscope method of presentation will be applied to a number of alternative types of r-f systems which will yield standing-wave information.

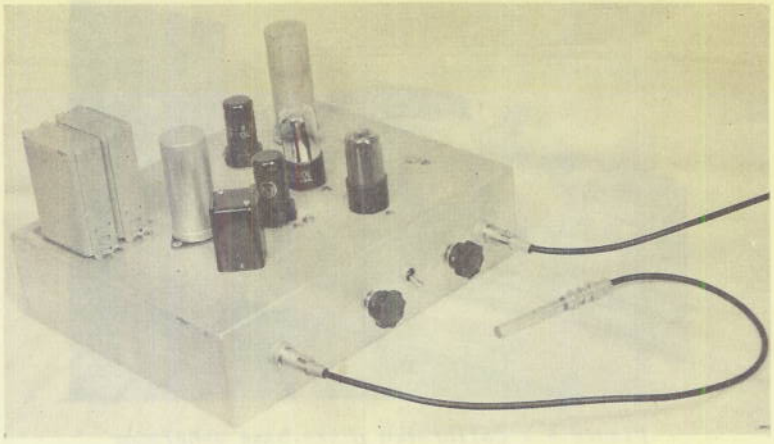

Figure 6a - Triggered phase-base generator

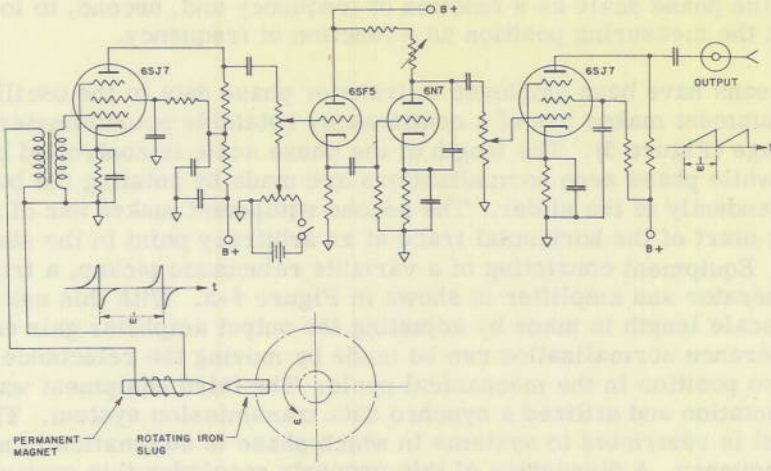

Figure 6b - Schematic sawtooth generator

Moving Detector Systems

One author (Reference 12) has given a description of a motor-driven, standing-wave detector utilizing oscilloscope presentation; the system makes use of a reciprocating detector motion on a straight section of line. Detector position is shown on the oscilloscope by means of a potentiometer scheme. A similar but alternative means of providing a motor drive is shown in Figure 7. In this system the detector probe is driven at constant angular velocity; the section of line under test is bent in a semicircle to follow the path of the probe. The phase-base generator used in this equipment was the variable reluctance pickup type.

Since both systems are modifications of conventional standing-wave instruments, the attainable accuracy should be comparable to that of a conventional detector. The mechanical features of these instruments, however, tend to limit their utility.

The reciprocating detector is subject to severe accelerations which tend to reduce the attainable accuracy when the frequency of the transmission line scan is sufficiently high to

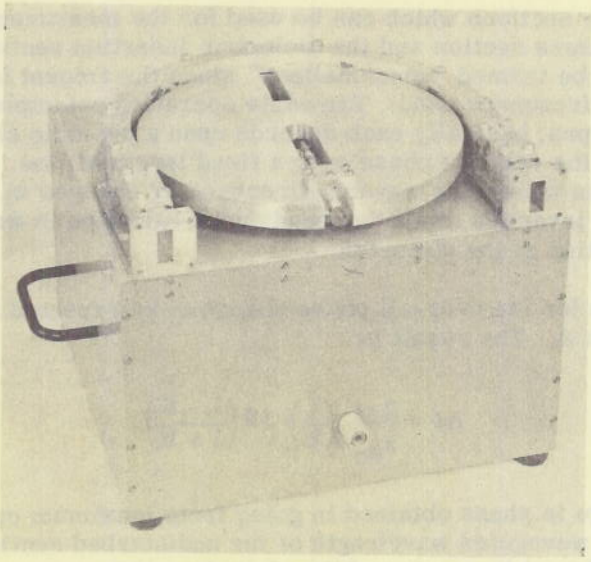

Figure 7 - Rotating standing-wave detector

produce good oscilloscope presentation. Motional noises are generated and tend to limit the minimum usable signal level. The rotating type detector, while not subject to the acceleration problems of the reciprocating system, does require a motional joint between the probe and output connector and has the further disadvantage of supplying information during only half of the period of rotation.

The rotating detector has one additional disadvantage which makes the system impractical for general use. Since the transmission line is bent into a semicircular arc, the minimum radius which can be used is limited by the reflections set up in the bend. To minimize such reflections the radius and hence the circumference over which the probe is active must be made large. Thus a large number of standing-wave maxima and minima are obtained at the detector output during a half revolution. If a pulsed source of r-f is used, the number of keying cycles per wavelength along the line at reasonable probe speeds is too small to delineate the standing-wave envelope with any degree of accuracy. At the longer wavelengths such difficulties can be overcome, particularly when coaxial lines are used. No attempt was made to utilize this equipment with a c.w. source of r-f, although it may be possible to utilize the a-c component of the detector output as a measure of the standing-wave ratio; the instrumentation required would seem to be prohibitive.

Both of these instrument types have a sufficient number of difficulties to make them impractical as laboratory tools.

Unnormalized, Fixed-Detector Systems

An alternative way of presenting the standing-wave conditions on a line by means of an oscilloscope is the use of a fixed detector and a continuously adjustable phase shifter to control the relative phase between incident and reflected waves. Many types of phase-shifter networks are available for use in such systems; several will be described in this section.

The characteristics of most phase-shifter networks make it impractical to compute phase scale information. As a consequence, such systems can be used only with scales which have been obtained in terms of a known load such as a short circuit.

Two phase-shifter sections which can be used for the measurement of standing waves are the waveguide squeeze section and the dielectric insertion section (Reference 13). Both of these systems may be termed "unnormalized" since the amount of phase shift produced is dependent upon the frequency used. The same operating principle is utilized in both of these phase-shifter types; basically each depends upon a periodic change in the waveguide wavelength to control the relative phase over a fixed length of line. The squeeze section utilizes the variation in waveguide wavelength caused by changes in the width of the waveguide. The dielectric insertion method depends upon variation in waveguide wavelength produced by the insertion of the dielectric.

An approximation for the over-all phase change to be expected from a squeeze section is derived in Appendix A. The result is

$$\Delta\phi = \frac{2\pi l}{\lambda_{g_o}} \left(\frac{1}{k}\right) \ln\left(\frac{1 - K}{1 + K}\right)$$

where $\Delta\phi$ is the change in phase obtained in going from maximum open to maximum closed conditions; λ_{g_o} is the waveguide wavelength of the undisturbed section of line; K is the amplitude of the deformation at the center of the slotted section.

A system utilizing the waveguide squeeze section is shown in Figure 8. The waveguide is oscillated by a motor with a cam arrangement. A potentiometer, whose shaft is connected to the cam drive, is used to generate the horizontal sweep voltage for the oscilloscope. Representative patterns obtained by the use of this equipment are shown in Figure 9.

The dielectric insertion method has been described by Kallmann along with an alternative means of presenting amplitude data (Reference 14); no attempt was made to obtain phase data with the equipment described in this article. An arrangement similar to that used on the squeeze section could be employed with this equipment. Oscilloscope patterns similar to those of the squeeze section would be obtained (Figure 9).

One difficulty was encountered in the presentation of phase with the squeeze-section system. Since the same r-f phase conditions are obtained at an arbitrary guide width, regardless of whether the section is opening or closing, one half of the pattern obtained is a mirror image of the other half. This phenomenon does not make it impossible to use the zero phase adjustment scheme outlined above but it does produce patterns which may be confusing to the operator. The possibility of eliminating one half of the sweep does exist, but the gain in pattern clarity can only be obtained at the expense of more complicated instrumentation in the sweep generating circuits. The final solutions to these problems were not actively sought since other phase-shifter methods indicated that simpler instrumentation techniques could be employed.

It should be noted that these two methods are applicable to waveguide transmission lines only. The dielectric insertion scheme becomes too cumbersome in coaxial lines because of the relatively slow change in wavelength caused by the insertion of a dielectric slab. No external variation in guide wavelength obtained in a manner similar to the squeeze section is possible for a transmission system which propagates principal waves. Phase-shifter networks which make use of variable lengths of line are impractical for mechanical reasons. These systems, therefore, have only limited application.

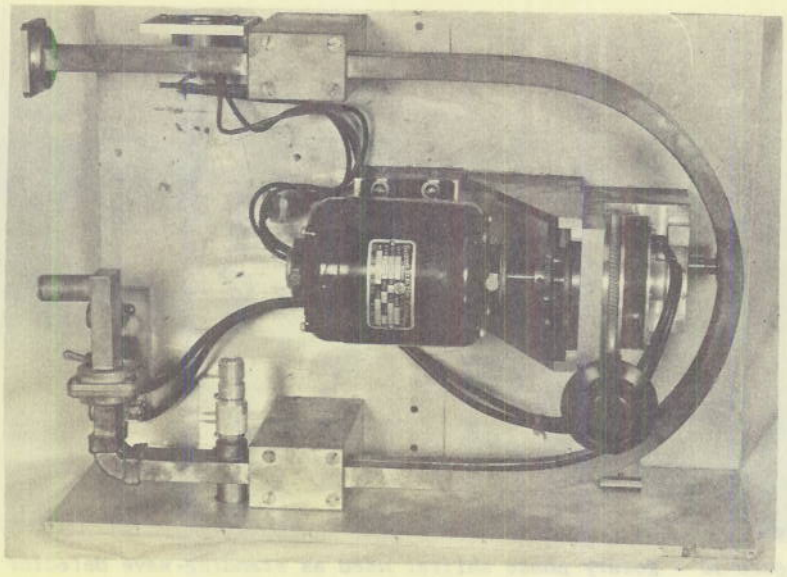

Figure 8 - Oscillating waveguide standing-wave detector

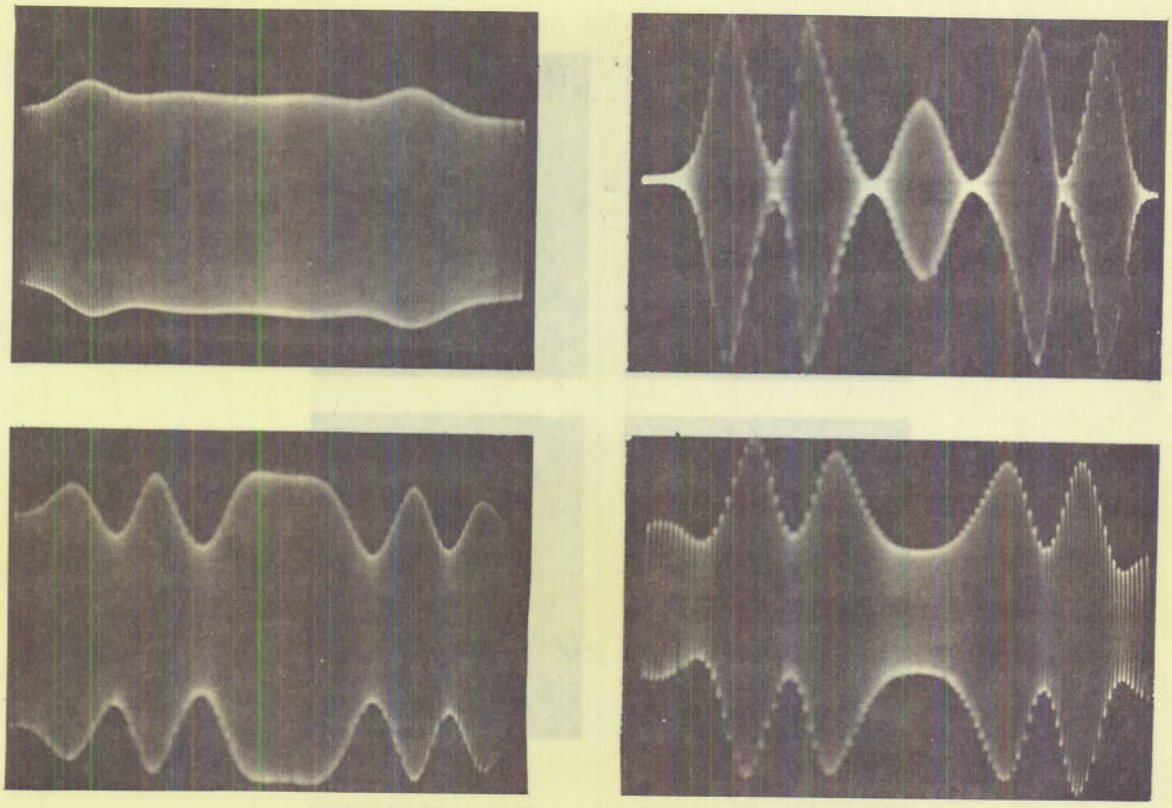

Figure 9 - Representative patterns of standing-waves - Oscillating waveguide standing-wave detector

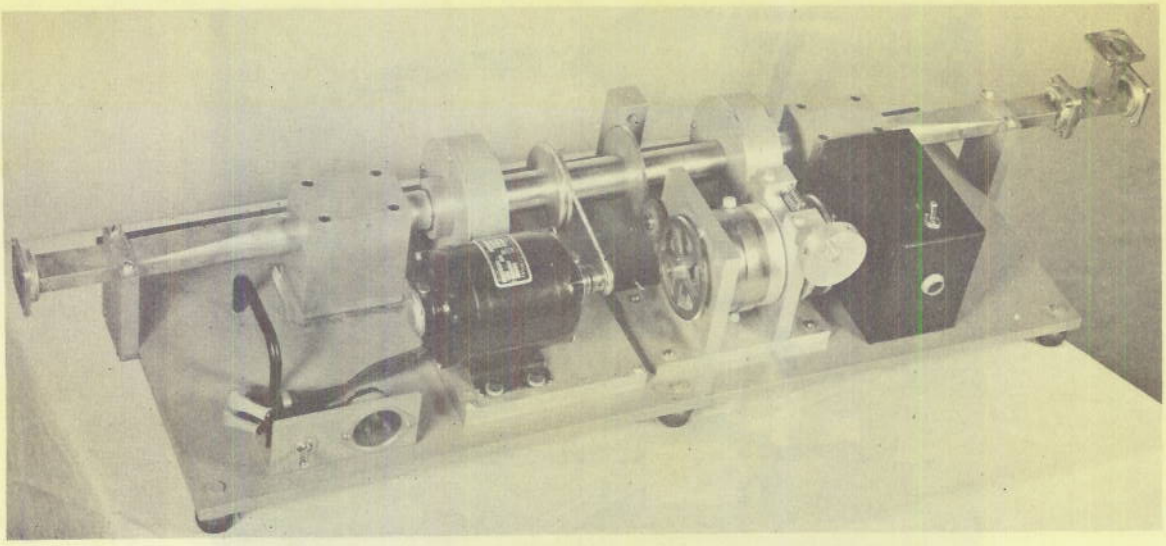

Figure 10 - Rotary phase shifter used as standing-wave detector

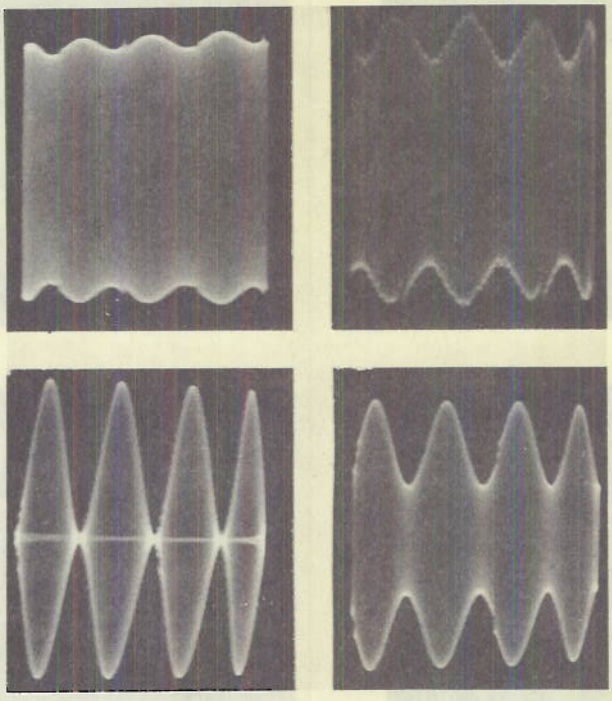

Figure 11 - Representative patterns of standing waves - Rotary phase shifter standing-wave detector

Normalized Fixed Detector Systems

A network in which the relative phase shift is independent of frequency and only dependent upon a mechanical adjustment may be called phase-normalized. A network which needs no phase-zero compensation as a function of frequency may be called phase-compensated. One phase-normalized system which can be used as a standing-wave detector is the rotary phase shifter (References 15, 16 and 17). In addition to providing a single linear phase scale at all frequencies, such a network makes it possible to utilize simple instrumentation in order to introduce phase-zero corrections.

Figure 10 illustrates a rotary phase shifter used as a standing-wave detector. The unit consists of the r-f line, drive motor, potentiometer time base generator (Figure 5) and the phase-zero correcting mechanism which is calibrated as a function of frequency. Figure 11 shows some typical oscilloscope patterns obtained with this equipment.

The center section is driven at a rate of 600 rpm while the r-f oscillator is keyed at 2000 cps. Thus 200 keying cycles are available during one sweep of the oscilloscope for the delineation of the standing-wave envelope. These values represent a reasonable compromise between pattern delineation, bolometer sensitivity and the retentivity of the oscilloscope image.

Relative phase as seen on the oscilloscope face may be controlled by rotating the body of the potentiometer, which carries a uniformly calibrated "A" scale (Figure 12). A "B" scale which can be adjusted and fixed in angular position carries the zero marker against which the "A" scale is compared. The "B" scale also carries graduations which are a function of frequency and are compared with a fixed marker on the equipment. The frequency ("B") scale is determined by the use of short-circuit conditions on the line, but the relative phase ("A") scale on the potentiometer can be obtained from computed values. In using the equipment to determine the phase of a test load, the "B" scale is adjusted to the proper value, then the potentiometer is rotated to give a minimum at the start of the pattern. The relative phase is obtained by reading the "A" scale appearing opposite the zero marker.

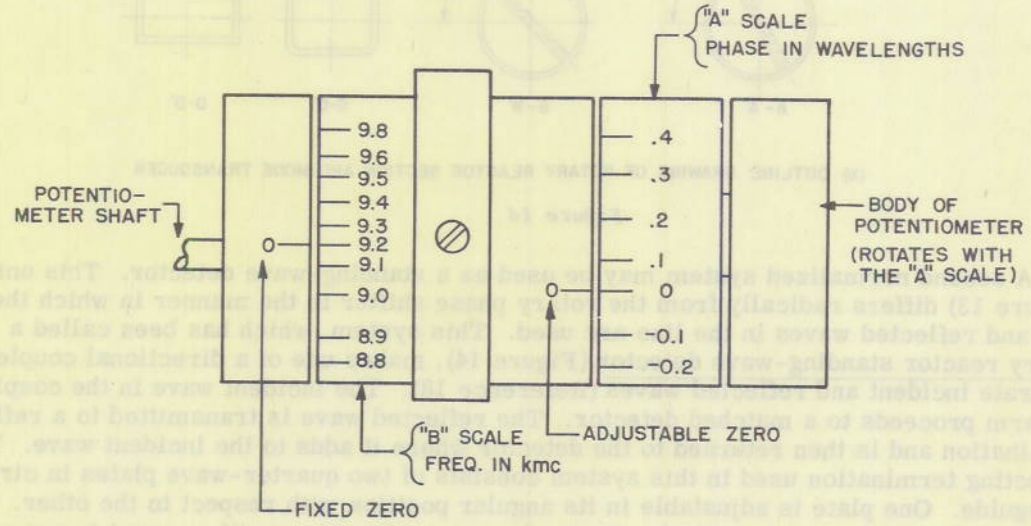

Figure 12 - Phase scale diagram
Rotary phase shifter standing-wave detector

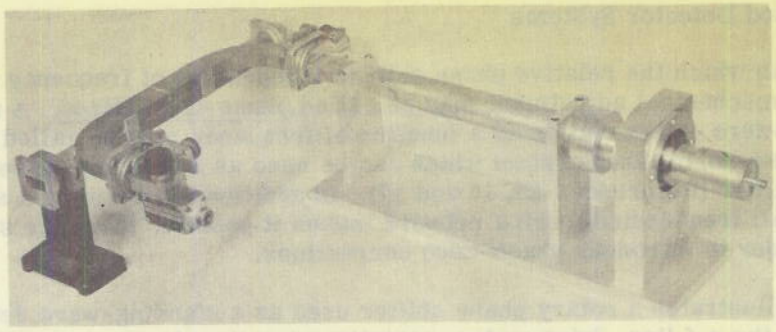

Figure 13 - Rotary reactor standing-wave detector

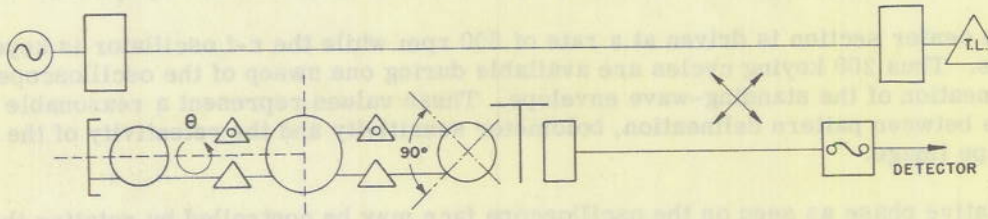

(a) SCHEMATIC - ROTARY REACTOR STANDING WAVE DETECTOR

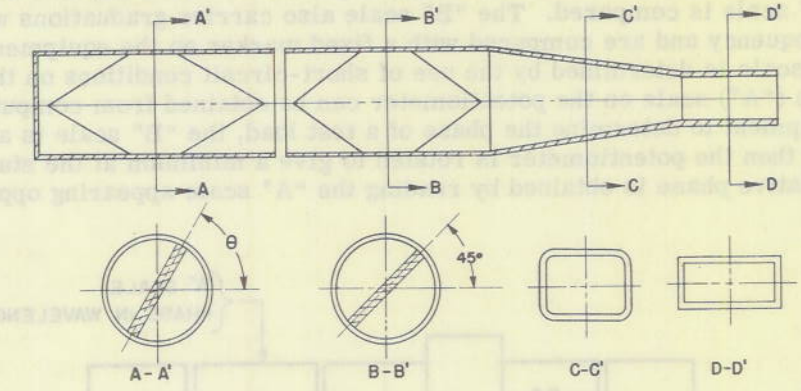

(b) OUTLINE DRAWING OF ROTARY REACTOR SECTION AND MODE TRANSDUCER

Figure 14

A second normalized system may be used as a standing-wave detector. This unit (Figure 13) differs radically from the rotary phase shifter in the manner in which the incident and reflected waves in the line are used. This system, which has been called a rotary reactor standing-wave detector (Figure 14), makes use of a directional coupler to separate incident and reflected waves (Reference 18). The incident wave in the coupler sidearm proceeds to a matched detector. The reflected wave is transmitted to a reflecting termination and is then returned to the detector where it adds to the incident wave. The reflecting termination used in this system consists of two quarter-wave plates in circular waveguide. One plate is adjustable in its angular position with respect to the other. Such a network produces a change in the phase of an emerging wave, with respect to one entering, which is directly proportional to the mechanical angle of the second quarter-wave plate (see Appendix B).

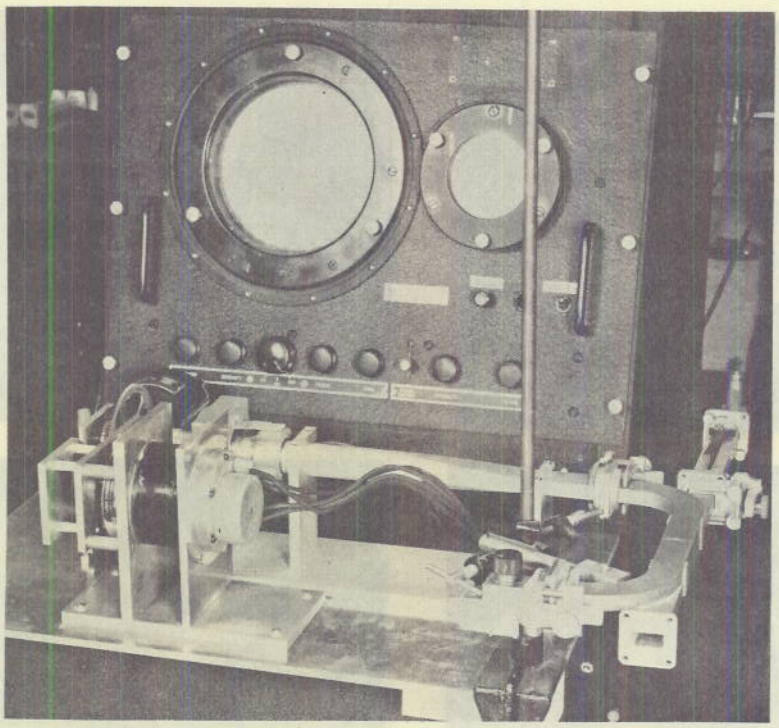

Figure 15 - Rotary reactor standing-wave detector instrumentation for polar coordinate presentation

The instrumentation required is similar for the rotary phase shifter when oscilloscope presentation is used; an equipment using polar coordinate presentation is shown in Figure 15. It uses a motor (geared down 30:1) to drive the rotary reactor. A 10 to 1 step-up is used to drive a synchro generator from the rotary reactor shaft. The yoke-positioning system in the oscilloscope is geared down 10:1 to follow the rotary reactor position. A long-persistance screen is used to provide sufficient retention at the low-speed for the rotary reactor drive. No provision was made to rotate the frame of the synchro to introduce the phase-zero correction. Representative patterns obtained with this equipment are shown in Figure 16.

Both systems just described make use of propagation in circular-cylindrical waveguide. In the first system all of the energy reaching the test load is made to pass through the rotary phase-shifter section. Thus when test loads other than those in cylindrical waveguide are used it is necessary to provide a well matched transition between the test equipment and the load. In the second system, however, only a small part of the energy incident upon the test load is used in the measuring circuits. No transition between the test equipment and load will be needed if a suitable directional coupler can be provided between the test line and cylindrical waveguide.

A number of measurements were made to compare the results obtained from the first of these equipments with those obtained with a standing-wave detector. Figure 17 illustrates some of the results obtained. It is evident that with the laboratory equipment available serious errors were encountered. An investigation of these errors showed that the dielectric sections in the cylindrical waveguide were departing quite radically from the ideal conditions needed for proper operation. A preliminary investigation of the operation of

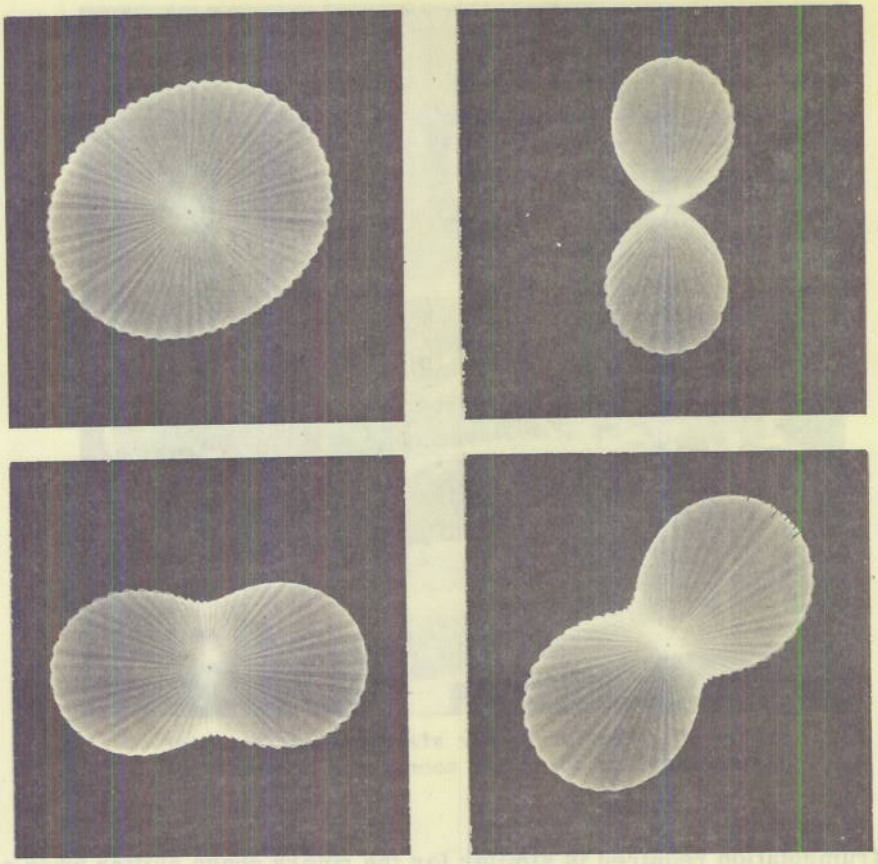

Figure 16 - Representative patterns of standing-waves rotary reactor standing wave detector

such dielectric plates indicates that they may, in theory, be made to have the desired properties over a wide range of frequencies; practical limitations are not expected to prevent major improvements in the operation of these units.

In terms of the instrumentation required and the type of presentation possible, these two systems seem to be quite satisfactory, and more nearly suitable to present needs than the other semi-automatic standing-wave instruments discussed. The rotary reactor instrument has errors introduced by the finite directivity of the directional coupler employed. Appendix C contains an analysis of the errors to be expected in such a system. In the laboratory equipment used, directional couplers of 30 db (d = 0.02 of Figures 22 and 23 in Appendix C) directivity were employed. The errors to be expected are thus ± 4 percent in measured standing-wave ratio. In the light of the difficulties encountered with the dielectric sections in the rotary phase shifter, only a qualitative confirmation of the operation of this equipment was obtained. Improved designs for directional couplers, which will soon be available, will limit the errors from this source to ± 1 percent or less. A diagram showing the performance of the rotary reactor section alone appears as Figure 19 in Appendix B.

SUMMARY AND CONCLUSIONS

Improved performance obtained with conventional slotted sections at X-band indicates that the methods employed could profitably be incorporated in the design of new laboratory

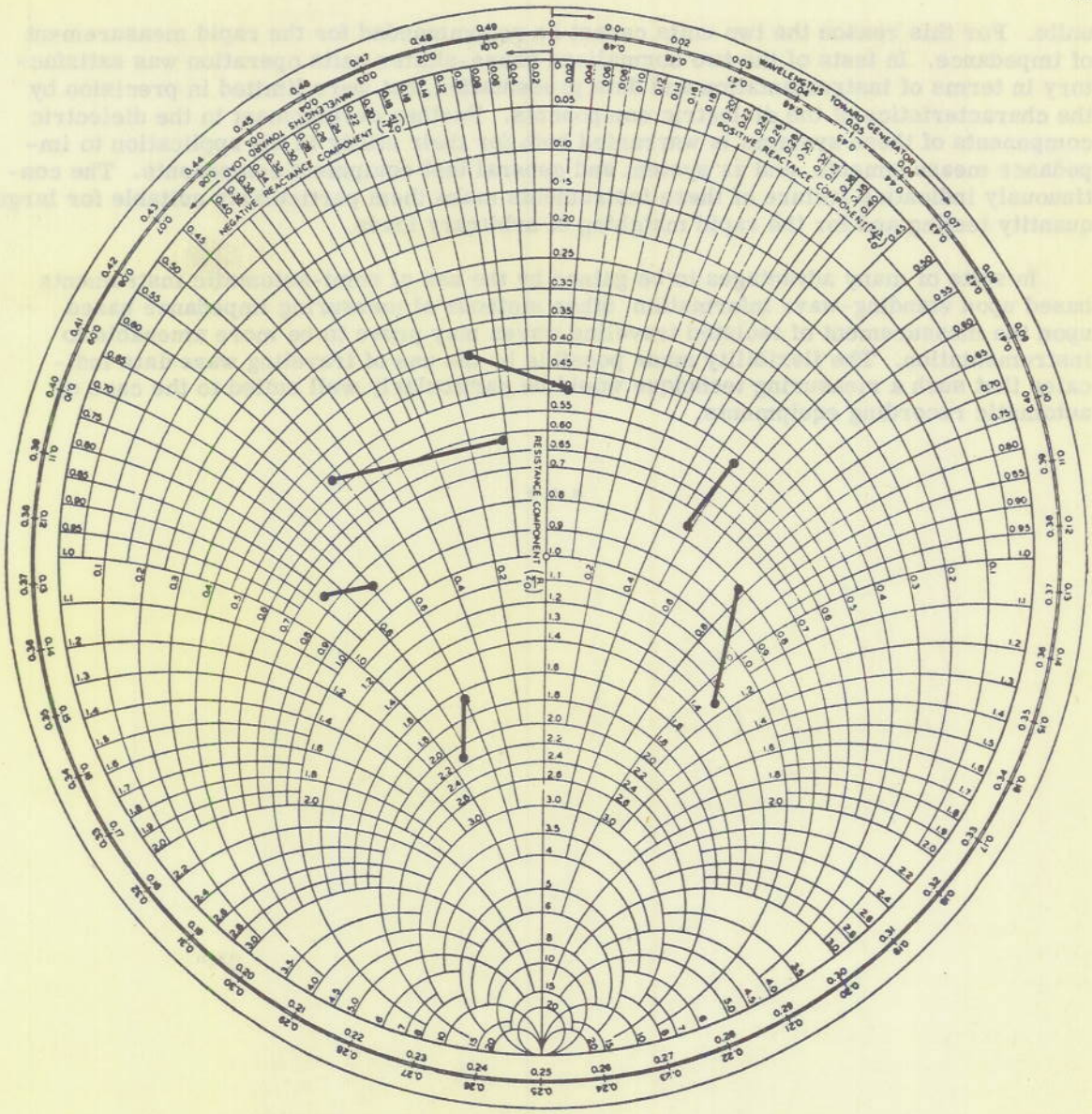

Figure 17 - Comparison of observed data - Standing-wave detector vs. rotary phase shifter

equipments for use in other frequency ranges. Further effort in this direction can be justified since slotted line equipments have possibilities for precision not realizable in other types of impedance measuring equipments. In the present form, on the other hand, standing-wave detectors too often compel the operator to make a compromise between the desired amount of data and that amount which can be obtained in a reasonable length of time.

Motorized standing-wave detectors do not seem to warrant further effort since they are limited by both electrical and mechanical difficulties. In addition they present problems of indication that can be solved more readily by the use of phase-shifter equipments.

The oscillating waveguide phase-shifter and the dielectric insertion scheme present difficulties in indication which can be solved easily by the use of normalized phase-shifter

units. For this reason the two units cannot be recommended for the rapid measurement of impedance. In tests of the two normalized phase-shifter units operation was satisfactory in terms of instrumentation and data presentation, but were limited in precision by the characteristics of the dielectric components. Further development in the dielectric components of these systems is warranted both for their utility in the application to impedance measurements, and as system and general test equipment components. The continuously indicating feature of these instruments make them particularly suitable for large quantity testing and for the rapid matching of arbitrary loads.

In spite of many advantages to be gained by the use of semi-automatic instruments based upon standing-wave information, other methods of measuring impedance based upon the measurement of isolated traveling waves may prove to be more amenable to instrumentation. The flexibility made possible by the use of traveling wave data indicates that such a measuring technique would be particularly well suited to the case of automatic recording equipments.

* * *

REFERENCES

1. Guillemin, E. A. "Communication Networks," Vol. II, Chap. I, Sect. 4, New York: J. Wiley, 1935.
2. Montgomery, C. G. "Technique of Microwave Measurements," Chap. VIII, New York: McGraw-Hill, 1947.
3. Gaffney, F. J. "Microwave Measurements and Test Equipment," Proc. of I.R.E., 34: 775-793, Oct. 1946.
4. Johnson, S. A. "Microwave Slotted Sections," Proc. of National Electronics Conference, 4: 222-32, Nov. 1948.
5. Wholey, W. B. and Eldred, W. N. A New Type of Slotted Line Section (Abstract), Proc. of National Electronics Conference, 4: 221, Nov. 1948.
6. Portmann, P. A. Survey of Generalized Impedance Measuring Techniques for the Microwave Frequencies; NRL Report R-3497 (Unclassified), June 28, 1949.
7. Altar, W., Hunter, L. P., and Marshall, F. B. "Probe Error in Standing-Wave Detectors," Proc. of I.R.E., 34: 33-44, Jan. 1946.
8. Tomiyasu, K. "Loading and Coupling Effects of Standing-Wave Detectors," Proc. of I.R.E., 37: 1405-9, Dec. 1949.
9. Altar, W. and Coltman, T. W. Microwave Impedance Plotting Device; Proc. of I.R.E., 35-7: 734-737, July 1947.
10. Ragan, G. L. "Microwave Transmission Circuits," Sect. 6.12, New York: McGraw-Hill, 1948.
11. Montgomery, C. G. "Technique of Microwave Measurements," Sect. 3.27, New York: McGraw-Hill, 1947.
12. Allen, P. J. "An Automatic Standing-Wave Detector," Proc. AIEE, 67-II: 1299-1302, Nov. 1948.
13. Ragan, G. L. "Microwave Transmission Circuits," Sect. 8.16, New York: McGraw-Hill, 1948.
14. Kallmann, H. E. "Standing-Wave Meter," Electronics, 20: 96-9, Jan. 1947.
15. Fox, A. G. "An Adjustable Waveguide Phase Changer," Proc. I.R.E., 35-12: 1489-1498, Dec. 1947.
16. Simmons, A. J. and Mayer, M. A. "X-Band Phase-Shifter," MIT, Research Laboratory of Electronics, Radar and Intelligence Group, Internal Laboratory Report III on Project Meteor.
17. Montgomery, C. G., Dicke, R. H., and Purcell, E. M. "Principles of Microwave Circuits, Sect. 10.8, New York: McGraw-Hill, 1948.
18. Riblet, H. J. and Saad, T. S. "A New Type of Waveguide Directional Coupler," Proc. I.R.E., 36-1: 61-64, Jan. 1948.

APPENDIX A

Approximation for the Phase-Shift of a Deformable Waveguide Section

The waveguide wavelength, λ_g, of an arbitrary line is given by

$$\lambda_g = \frac{\lambda}{\sqrt{1 - (\lambda / \lambda_{co})^2}} \tag{1-A}$$

where λ is the free space wavelength. For a rectangular waveguide λ_{co}, the cutoff wavelength is

$$\lambda_{co} = 2a_o \tag{2-A}$$

where a_o is the internal broad dimension. If λ_c is made variable by a change in the dimension a_o, there will thus be a corresponding change in waveguide wavelength.

An automatic phase-shifter section may be made by slotting a length of rectangular waveguide in the center of the broad face over a length l and compressing or expanding the center of the section in a periodic manner (see Figure 18).

Let a_1 be the internal dimension at the mid-point of the slot length when the section is fully compressed. The periodic variation, a, in the width may then be written

$$a = a_o (1 - K \sin \alpha t) \tag{3-A}$$

where K is given by

$$K = \frac{a_o - a_1}{a_o}, \tag{4-A}$$

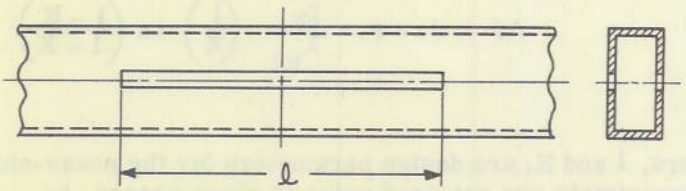

a. OUTLINE OF PHASE SHIFTER SECTION

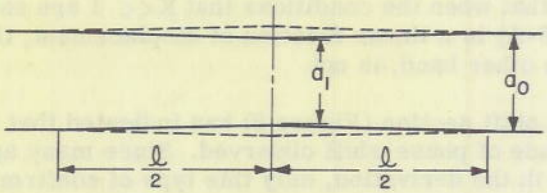

b. INTERNAL WAVEGUIDE DIMENSIONS

Figure 18 - Waveguide squeeze section phase shifter

and α is the frequency of the mechanical oscillation.

The value, a, may be used to obtain λ_c and λ_g. The equation resulting from a substitution of 3-A into 2-A and 2-A into 1-A may be written as

$$\lambda_g = \frac{\lambda}{\sqrt{1-\left(\frac{\lambda}{\lambda_{co}}\right)^2}} \quad (1 - K \sin \alpha t) \tag{5-A}$$

after assuming that terms in K and K^2 in the denominator can be neglected. In Equation 5-A, $\lambda_{co} = 2a_o$, so that this equation may be written as

$$\lambda_g = \lambda_{go} \quad (1 - K \sin \alpha t) \tag{6-A}$$

where λ_{go} is the waveguide wavelength of the undisturbed line section.

Over an element of length dx, the phase-shift is given by

$$d\phi = \frac{2\pi}{\lambda_g} \, dx. \tag{7-A}$$

If it is assumed that the waveguide is deformed in width linearly from zero to K over the range x = 0 to x = $l/2$, and from K to zero over the range x = $l/2$ to x = l, a simple relation is obtained which relates the waveguide wavelength at any point x along the slot to the guide wavelength at x = $l/2$. A simple integration over the length, l, then yields the phase-shift of the section as a function of the time-varying parameter sin α t. The result is

$$\phi = -\frac{2\pi l}{\lambda_{go}} \quad \frac{\ln(1 + K \sin \alpha t)}{K \sin \alpha t}. \tag{8-A}$$

The difference in phase introduced by the compression and expansion may be found by taking the difference of the two values of phase obtained by setting sin αt = $\pm$ 1. Thus,

$$\Delta\phi = \phi_2 - \phi_1 = \frac{2\pi l}{\lambda_{go}} \left(\frac{l}{K}\right) \ln\left(\frac{1 - K}{1 + K}\right). \tag{9-A}$$

The parameters, l and K, are design parameters for the phase-shift section, and can thus be used to approximate any required value of phase change, $\Delta\phi$.

It is of interest to note that when the conditions that $K << 1$ are satisfied, the waveguide wavelength (Equation 6-A) is a linear function of displacement; the phase-shift introduced (Equation 8-A), on the other hand, is not.

The design of the phase-shift section (Figure 8) has indicated that this formula gives the correct order of magnitude of phase-shift observed. Since many approximations to the physical situation are made in the derivation, only this type of confirmation is valid.

* * *

APPENDIX B

Analysis of a Reflecting Phase-Shift Network (Rotary Reactor)

Following the notation used by Montgomery, Dicke and Purcell (Reference 17) in analyzing the rotary phase-shifter, the rotary reactor network (Figure 14-b) may be analyzed in the following manner:

The scattering matrix of a circular section of waveguide whose output terminals are rotated 45^{0} with respect to the input terminals is given by

$$S_1 = \frac{e^{j\varphi_1}}{\sqrt{2}} \begin{bmatrix} 0 & 0 & 1 & 1 \\ 0 & 0 & -1 & 1 \\ 1 & -1 & 0 & 0 \\ 1 & 1 & 0 & 0 \end{bmatrix} \tag{1-B}$$

In passing through the first quarter-wave plate the scattering matrix, S_1, is transformed to S_2 in which the fourth row and fourth column are multiplied by -j and the phase advances from ϕ_1 to ϕ_2. If the axis of the second quarter-wave plate is at an angle θ with respect to the first, S_2 may be transformed to this new orientation:

$$S_2' = \tilde{T}\, S_2\, T = \frac{e^{j\phi_2}}{\sqrt{2}} \begin{bmatrix} 0 & 0 & e^{-j\theta} & -je^{-j\theta} \\ 0 & 0 & -e^{j\theta} & -je^{j\theta} \\ e^{-j\theta} & -e^{j\theta} & 0 & 0 \\ -je^{-j\theta} & -je^{j\theta} & 0 & 0 \end{bmatrix} \tag{2-B}$$

where $\tilde{T}$ is the transpose of T, and T is given by:

$$T = \begin{bmatrix} 1 & 0 & 0 & 0 \\ 0 & 1 & 0 & 0 \\ 0 & 0 & \cos\theta & -\sin\theta \\ 0 & 0 & \sin\theta & \cos\theta \end{bmatrix} \tag{3-B}$$

In going through the second quarter-wave plate the change in S_2' is again given effectively by multiplying the fourth row and fourth column by -j; thus

$$S_3 = \frac{e^{j\phi_3}}{\sqrt{2}} \begin{bmatrix} 0 & 0 & e^{-j\theta} & -e^{-j\theta} \\ 0 & 0 & -e^{j\theta} & -e^{j\theta} \\ e^{-j\theta} & -e^{j\theta} & 0 & 0 \\ -e^{-j\theta} & -e^{j\theta} & 0 & 0 \end{bmatrix}. \tag{4-B}$$

If the input to the network is given by the column vector,

$$a = \begin{bmatrix} 1 \\ 0 \\ 0 \\ 0 \end{bmatrix}, \tag{5-B}$$

the output $b = S_3\, a$ becomes

$$b = \frac{e^{j\phi_3}}{\sqrt{2}} \begin{bmatrix} 0 \\ 0 \\ e^{-j\theta} \\ -e^{-j\theta} \end{bmatrix} \tag{6-B}$$

If now these waves are reflected by means of a short circuit on the end of the line, a new input to the circuit may be formed by changing the sign of the output b; thus,

$$a' = -b = \frac{e^{j\phi_3}}{\sqrt{2}} \begin{bmatrix} 0 \\ 0 \\ -e^{-j\theta} \\ e^{-j\theta} \end{bmatrix} \tag{7-B}$$

If this input is applied to the circuit the resulting output b' will be given by

$$b' = S_3 a', \tag{8-B}$$

or by

$$b' = -e^{j(2\phi_3 - 2\theta)} \begin{bmatrix} 1 \\ 0 \\ 0 \\ 0 \end{bmatrix}. \tag{9-B}$$

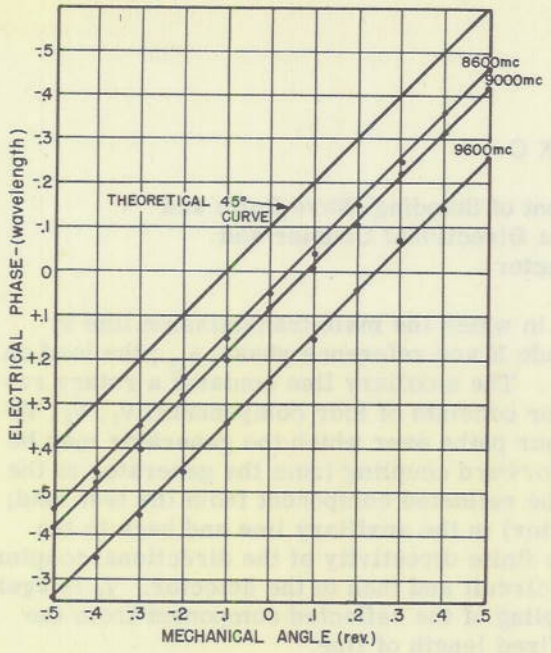

Figure 19 - Rotary reactor - test data

The output, b′ is therefore a linearly polarized wave which emerges from the terminals at which the input, a is supplied, but the phase of the emerging wave is a function of the relative angle (θ) between the two quarter-wave plates. Figure 19 shows the experimental results obtained with this unit at a number of frequencies.

One additional feature of this instrument may be mentioned. In place of the reflecting termination at the end of the line (i.e., the short circuit) it is possible to place a termination which only reflects a fraction of the power incident upon it. If this reflecting termination can be arranged to vary the amount of reflection without a corresponding phase-shift, it would be possible to synthesize a load whose reflection coefficient magnitude and phase can be controlled independently. Such a device would be useful in many instrumentation problems.

* * *

APPENDIX C

Systematic Errors in the Measurement of Standing-Wave Ratio and Phase in Equipments Employing a Directional Coupler and Rotary Reactor

Consider the system shown in Figure 14-a in which the main transmission line is excited by a generator having a voltage magnitude E and reference phase, ϕ_0 ; the load on this line has a complex reflection coefficient Γ . The auxiliary line contains a rotary reactor and a detector. The voltage at the detector consists of four components, V_1 , V_2 , V_3 and V_4 ; these are obtained by considering the four paths over which the generator may be coupled to the detector. Thus V_1 is the direct forward coupling from the generator to the detector. V_2 is obtained by direct coupling of the reflected component from the test load; it travels to the reflecting circuit (Rotary Reactor) in the auxiliary line and back to the detector. V_3 is an undesirable signal due to the finite directivity of the directional coupler; the path is from the main line to the reflecting circuit and then to the detector. V_4 is again due to the finite directivity and is the back coupling of the reflected component from the test load; it feeds the detector directly over a fixed length of line.

If l is the length of transmission line between the generator and the test load, m the length of line between the rotary reactor and the detector, and if the directional coupler is located in the center of each of these line lengths, the voltage components at the detector may be written as

$$\begin{aligned} V_1 &= E \quad e^{j\left[\frac{\beta}{2}(l+m)+\phi_0\right]} \\ V_2 &= E\Gamma \quad e^{j\left[\frac{3\beta}{2}(l+m)+\phi_0+2\theta\right]} \\ V_3 &= Ed \quad e^{j\left[\frac{\beta}{2}(l+3m)+\phi_0+2\theta\right]} \\ V_4 &= Ed\Gamma \quad e^{j\left[\frac{\beta}{2}(3l+m)+\phi_0\right]} \end{aligned} \tag{1-C}$$

The angle θ is the mechanical angular position of the rotary reactor, and d is the directivity coefficient of the directional coupler and is assumed to be real.

The detector voltage will then be

$$V = V_1 + V_2 + V_3 + V_4. \tag{2-C}$$

A normalized detector voltage, v, may be obtained by setting

$$v = \frac{V}{E\, e^{j\left[\frac{\beta}{2}(l+m)+\phi_0\right]}} = 1 + \Gamma e^{j\left[\beta(l+m)+2\theta\right]} + d\, e^{j\left[\beta m+2\theta\right]} + \Gamma d e^{j\beta l}. \tag{3-C}$$

If the substitutions $\beta m = \phi_1$; $\beta l = \phi_2$ and the complex reflection coefficient Γ is written in the polar form as $|\Gamma|\, e^{j\theta_L}$, the right-hand member of Equation 3-C may be put in the form

$$v = 1 + |\Gamma|\, d\, e^{j\vartheta} + e^{j(\phi_1+2\theta)}\,(d + |\Gamma| e^{j\vartheta}) \tag{4-C}$$

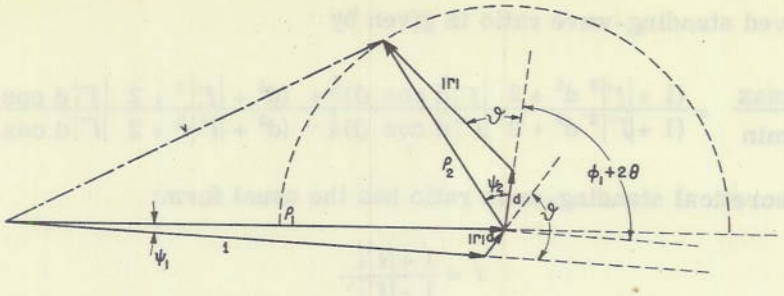

(a) GENERAL VECTOR RELATIONS

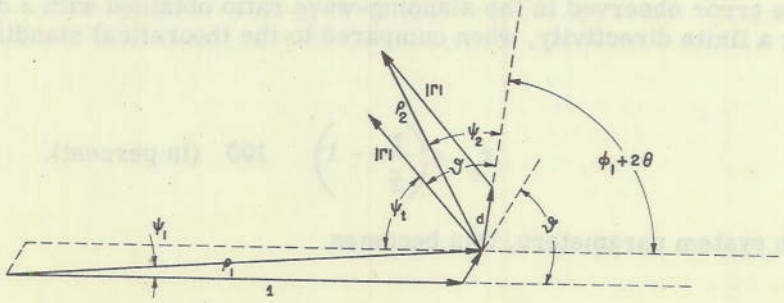

(b) PHASE ERROR RELATIONS

Figure 20 - Vector diagram of the detector response in a directional coupler-rotary reactor standing-wave detector system

where $\vartheta = \phi_2 + \theta_L$.

Standing-Wave Ratio Error

Equation 4-C is shown as a vector relation in Figure 20 (a). From the diagram it may be seen that

$$v_{max} = |\rho_1| + |\rho_2|$$

$$v_{min} = |\rho_1| - |\rho_2| . \qquad (5\text{-C})$$

The values for $|\rho_1|$ and $|\rho_2|$ may also be obtained from the diagram; thus,

$$|\rho_1| = \left|1 + |\Gamma|\, d\, e^{j\vartheta}\right|$$

$$|\rho_2| = \left|(d + |\Gamma|\, e^{j\vartheta}) e^{(j\phi_1 + 2\theta)}\right| . \qquad (6\text{-C})$$

The equations for v_{max} and v_{min}, after simplification, may be written as

$$v_{max} = (1 + |\Gamma|^2 d^2 + 2|\Gamma| d \cos\vartheta)^{\frac{1}{2}} + (d^2 + |\Gamma|^2 + 2|\Gamma| d \cos\vartheta)^{\frac{1}{2}}$$

$$v_{min} = (1 + |\Gamma|^2 d^2 + 2|\Gamma| d \cos\vartheta)^{\frac{1}{2}} - (d^2 + |\Gamma|^2 + 2|\Gamma| d \cos\vartheta)^{\frac{1}{2}} . \qquad (7\text{-C})$$

The observed standing-wave ratio is given by

$$r = \frac{V_{max}}{V_{min}} = \frac{(1 + |\Gamma|^2 d^2 + 2 |\Gamma| d \cos \vartheta)^{\frac{1}{2}} + (d^2 + |\Gamma|^2 + 2 |\Gamma| d \cos \vartheta)^{\frac{1}{2}}}{(1 + |\Gamma|^2 d^2 + 2 |\Gamma| d \cos \vartheta)^{\frac{1}{2}} - (d^2 + |\Gamma|^2 + 2 |\Gamma| d \cos \vartheta)^{\frac{1}{2}}}. \quad (8\text{-C})$$

If $d = 0$, the theoretical standing-wave ratio has the usual form:

$$\bar{r} = \frac{1 + |\Gamma|}{1 - |\Gamma|}. \quad (9\text{-C})$$

When $d \neq 0$, the error observed in the standing-wave ratio obtained with a directional coupler having a finite directivity, when compared to the theoretical standing-wave ratio, is given by

$$r_\epsilon = \left(\frac{r}{\bar{r}} - 1\right) \quad 100 \quad \text{(in percent)}. \quad (10\text{-C})$$

In terms of the system parameters, this becomes

$$r_\epsilon = 100 \left[\left(\frac{1 - |\Gamma|}{1 + |\Gamma|}\right) \frac{(1 + |\Gamma|^2 d^2 + 2|\Gamma| d \cos \vartheta)^{\frac{1}{2}} + (d^2 + |\Gamma|^2 + 2 |\Gamma| d \cos \vartheta)^{\frac{1}{2}}}{(1 + |\Gamma|^2 d^2 + 2|\Gamma| d \cos \vartheta)^{\frac{1}{2}} - (d^2 + |\Gamma|^2 + 2 |\Gamma| d \cos \vartheta)^{\frac{1}{2}}} - 1\right] \text{(in percent)}. \quad (11\text{-C})$$

Phase Measurement Error

The vector relations involved in the determination of phase errors are shown in Figure 20 (b). From this diagram two equations are obtained, one, the measured phase angle (ψ_m) and two, the expected phase angle with perfect directivity (ψ_t); these are

$$\begin{aligned} \psi_m + \psi_2 + \phi_1 + 2\theta &= \pi + \psi_1 \\ \psi_t + \vartheta + \phi_1 + 2\theta &= \pi \end{aligned} \quad . \quad (12\text{-C})$$

The error in measured phase is given by

$$\theta_\epsilon = \psi_m - \psi_t . \quad (13\text{-C})$$

Substituting the values from equation 12, there is obtained

$$\theta_\epsilon = \psi_1 - \psi_2 + \vartheta . \quad (14\text{-C})$$

The values of ψ_1 and ψ_2 may be obtained from Figure 20 (a):

$$\psi_1 = \tan^{-1} \frac{|\Gamma| d \sin \vartheta}{1 + |\Gamma| d \cos \vartheta} \quad (15\text{-C})$$

$$\psi_2 = \tan^{-1} \frac{|\Gamma| \sin \vartheta}{d + |\Gamma| \cos \vartheta} . \quad (16\text{-C})$$

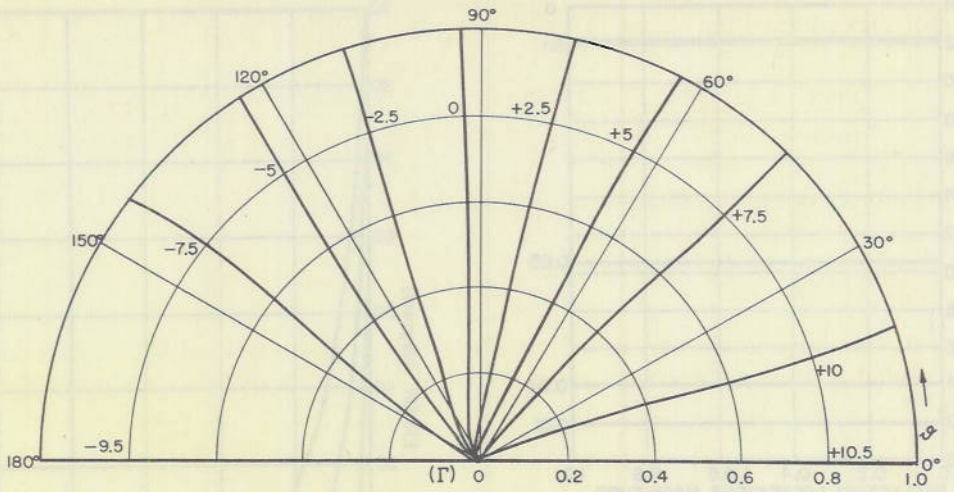

Figure 21A - Contours of constant standing-wave ratio error (%) (d = .05)

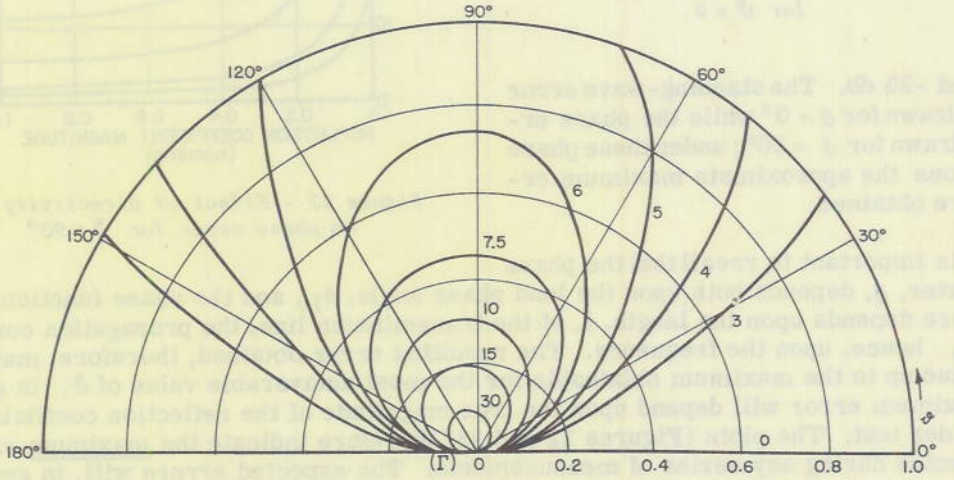

Figure 21B - Contours of constant phase error (deg.) (d = .05)

When these values are substituted in Equation (14-C) the result may be simplified to read

$$\theta_\epsilon = \tan^{-1} \frac{(d^2 - 1)\,|\Gamma| \sin\vartheta}{(1 + |\Gamma|^2)\,d + (d^2 + 1)\,|\Gamma| \cos\vartheta} + \vartheta \,. \qquad (17\text{-C})$$

The errors to be expected from the equipment as calculated from the error relations (Equations 11-C and 17-C) are illustrated in Figures 21(a) and 21(b). The first of these shows constant standing-wave ratio error contours while the second shows constant angular error contours. Both diagrams are plotted over the reflection coefficient plane, and thus give the expected measurement error for any passive load. The magnitude of errors illustrated are those obtained for directional coupler having a directivity of -26 db. Such a directivity is realizable and capable of being improved upon.

Figures 22 and 23 show the effect of directivity upon the standing-wave ratio and phase errors. The curves are drawn for directional couplers having directivities of -40, -34,

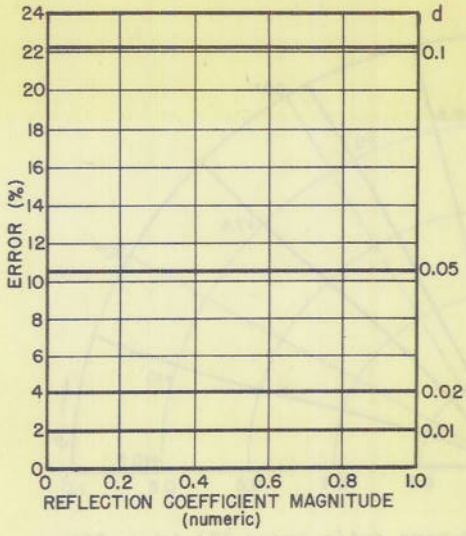

Figure 22 - Effect of directivity (d) on standing-wave ratio error for $\vartheta = 0$

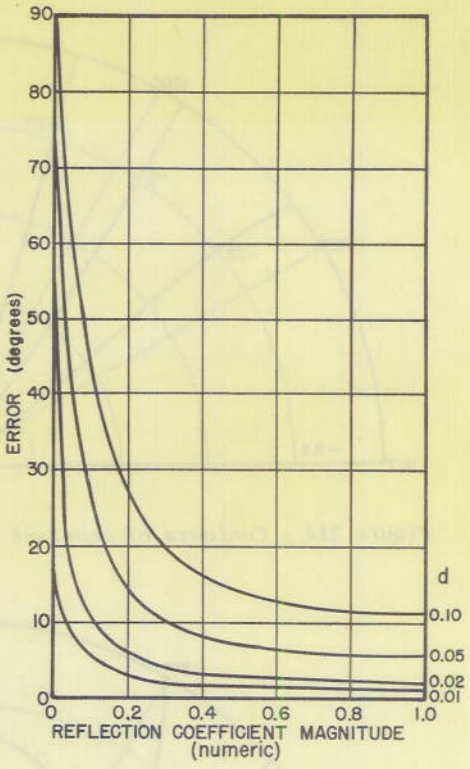

Figure 23 - Effect of directivity (d) on phase error for $\vartheta = 90^{o}$

-26, and -20 db. The standing-wave error plot is drawn for $\vartheta = 0^{o}$ while the phase error is drawn for $\vartheta = 90^{o}$; under these phase conditions the approximate maximum errors are obtained.

It is important to recall that the phase parameter, ϑ, depends both upon the load phase angle, θ_L, and the phase function, ϕ_2, and therefore depends upon the length, l, of the transmission line, the propagation constant, β, and, hence, upon the frequency. The resulting error obtained, therefore, may have any value up to the maximum obtainable for the most unfavorable value of ϑ. In general, the maximum error will depend upon the true magnitude of the reflection coefficient of the load under test. The plots (Figures 22 and 23) therefore indicate the maximum errors to be expected during any series of measurements. The expected errors will, in general, be less than those indicated by the graphs for any series of tests and test conditions.

* * *